Sensors and Materials, Vol. 37, No. 6 (2025) 2507–2511
MYU Tokyo

S & M 4070

Study and Fabrication of Ga_2O_3 Thin Films Using Thermal Evaporation

Ching-Fang Tseng,[1*] Ya-Chin Chiang,[1] and Cheng-Hsing Hsu[2]

[1]Department of Electronic Engineering, National United University,
No. 2 Lien-Da, Nan-Shih Li, 26063, Miao-Li 360302, Taiwan
[2]Department of Electrical Engineering, National United University,
No. 2 Lien-Da, Nan-Shih Li, 26063, Miao-Li 360302, Taiwan

(Received January 18, 2025; accepted May 29, 2025)

Keywords: Ga_2O_3 thin films, thermal evaporation, electrical properties

In this study, we deposited Ga_2O_3 thin films on Si substrates by thermal evaporation and investigated the effects of surface morphology and electrical properties on various thermal treatments. Diffraction patterns indicated that the annealed films had a polycrystalline microstructure and that the grain size of Ga_2O_3 thin films increased with annealing temperature. These results indicate that suitable processing parameters are beneficial in terms of improving the microstructure and electrical performance of Ga_2O_3 thin films. The Ga_2O_3 thin films are suitable for use as a thin-film transistor or sensor.

1. Introduction

Ga_2O_3 has attracted attention because of its chemical stability and excellent material properties, such as its ultrawide energy gap (4.9 eV) and extremely high breakdown field strength (approximately 8 MV/cm). Various β-Ga_2O_3-based devices, such as Schottky barrier diodes, metal oxide field effect transistors (MOSFET), oxygen sensors, and ultraviolet light detectors, have been fabricated.(1) However, β-Ga_2O_3 has a lower thermal conductivity (10–25 W/m·K) than SiC and GaN, rendering thermal management a key challenge for β-Ga_2O_3 power devices.(2–5) In addition, for sensor application, the resistivity of Ga_2O_3 changes with oxygen concentration in the film, and an oxygen sensor was made on the basis of this result.(6) Moreover, the elusiveness of efficient p-type β-Ga_2O_3 materials has limited the application of Ga_2O_3. Therefore, β-Ga_2O_3 bipolar components with lower on-resistance and power consumption must be developed to improve their performance in high-power applications.(5)

In this study, we performed vacuum thermal evaporation deposition. Specifically, aluminum oxide was first deposited on a silicon substrate; then, gallium oxide was deposited and annealed at different temperatures in air. The fabricated material was evaluated on the basis of X-ray diffraction (XRD), scanning electron microscopy (SEM), sheet resistance, and *I*–*V* data.

*Corresponding author: e-mail: cftseng@nuu.edu.tw
https://doi.org/10.18494/SAM5560

ISSN 0914-4935 © MYU K.K.
https://myukk.org/

2. Experimental Procedures

A vertical furnace tube was used for thermal evaporation. First, the silicon substrate was placed above the furnace tube, the aluminum ingot was placed in the tungsten boat, and the tungsten boat was placed in the furnace tube. After the pressure in vacuum reached 7×10^{-5} Torr, the electrode output current (Vr) was adjusted to completely melt the aluminum ingot on the tungsten boat; then, the baffle was opened for evaporation over 3 min. Subsequently, gallium was placed in the tungsten boat, and the preceding steps were repeated for further evaporation. Finally, the test pieces were annealed in atmosphere at 350–600 °C. An XRD analyzer was used to determine the crystallinity of the 20–60° thin film on the annealed test piece, a scanning electron microscope was used to observe the surface morphology, and a four-point probe was used to measure the resistance for calculations of resistivity. The material was also evaluated in terms of its *I*–*V* curve.

3. Results and Discussion

Figure 1 shows the XRD patterns of Ga_2O_3 films annealed at different temperatures for 2 h. The diffraction patterns were largely invariant to annealing temperatures with similar

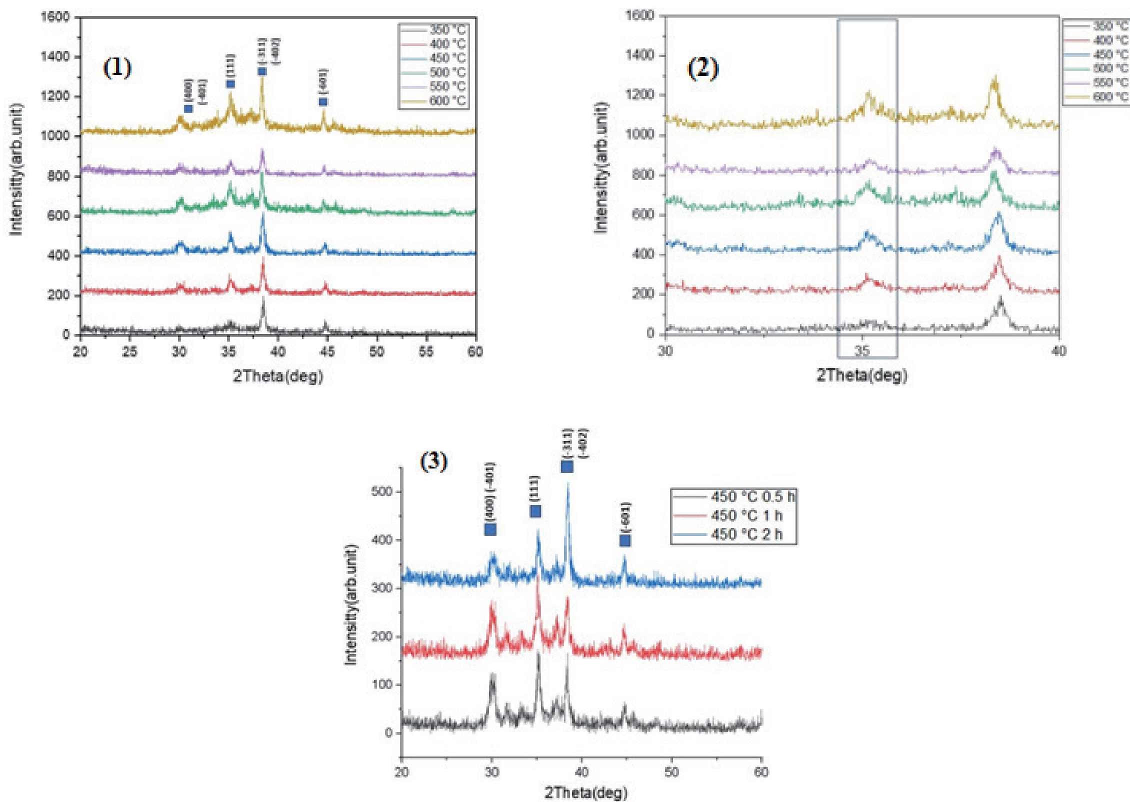

Fig. 1. (Color online) XRD patterns of Ga_2O_3 films for various annealing temperatures and times.

crystallization results, and only slight changes in peak intensity and width were noted. Diffraction peaks were observed at 30, 35, 38 and 44° for the (400), (−401), (111), (−311), (−402), and (−601) phases, indicating that Ga_2O_3 was polycrystalline. The summed average of the first three peaks at different temperatures indicated that annealing at 450 °C over 2 h was optimal. In general, higher annealing temperatures corresponded to a higher and wider peak at 35°. Given that 35° corresponds to the Al_2O_3 phase (211), the wider peak may have been caused by the effects of the Al_2O_3 phase on various thermal treatments.

Findings from high-resolution thermal field emission SEM on the microstructures of Ga_2O_3 thin films are shown in Fig. 2. More small particles were present on large particles at higher annealing temperatures, with nearly no small particles at the lowest temperature. Figure 3 shows a cross-sectional view of a Ga_2O_3 film. The particles were large at 350 °C, and the cross section of the film became thicker as more small particles adhered to larger particles at higher temperatures.

A four-point probe was used to determine the resistivity of a Ga_2O_3 film and the results are presented in Table 1. The resistivity is affected by the defect, grain size, and crystallinity. According to the XRD and SEM patterns, a lower porosity and a higher grain size resulted in a lower resistivity. In addition, the XRD intensities of the Ga_2O_3 peaks increased with annealing temperature, which indicates that the microstructure and phase of Ga_2O_3 affect the resistivity of

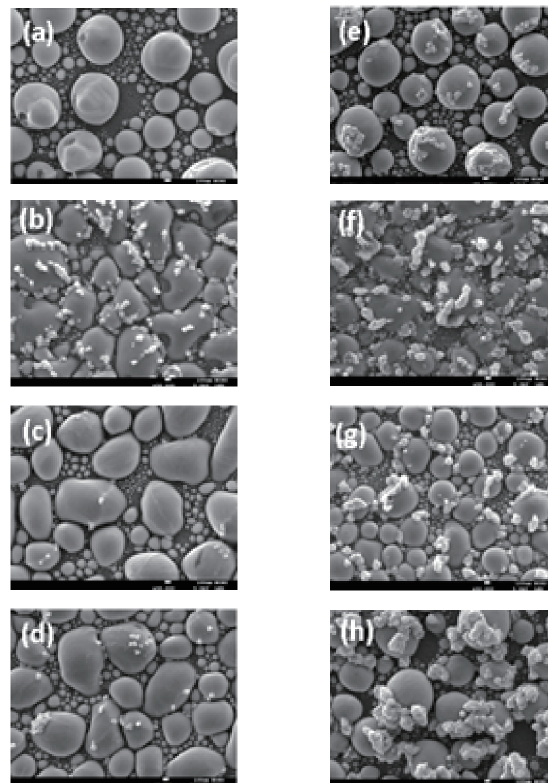

Fig. 2. SEM images of Ga_2O_3 films at various annealing temperatures and times.

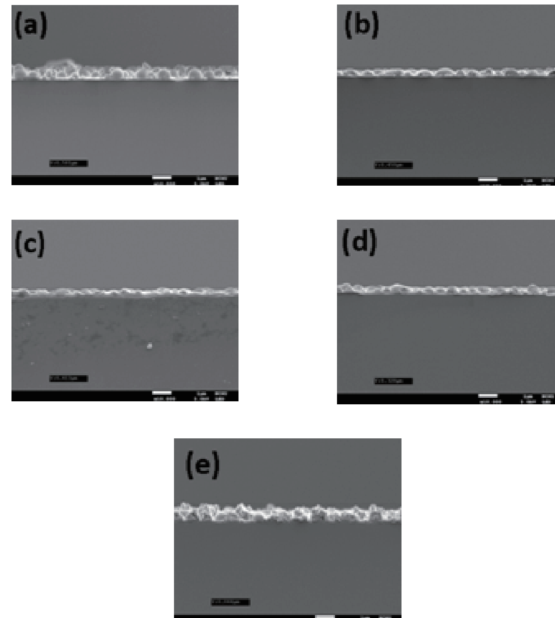

Fig. 3. Cross-sectional SEM images of Ga_2O_3 films at various annealing temperatures and times.

Table 1
Thickness values, resistance, and resistivity of Ga_2O_3 films at various annealing temperatures and times.

Annealing temperature and time	Thickness (μm)	Resistance (Ω)	Resistivity (μΩ/cm)
350 °C/2 h	0.581	0.107	32.97
450 °C/0.5 h	0.450	0.16	38.18
450 °C /1 h	0.413	0.14	30.66
450 °C/2 h	0.328	0.15	26.09
600 °C/ 2 h	0.844	0.450	201.40

Ga_2O_3 films. The resistivity was lowest (at 26.09 μΩ/cm) when the films were annealed at 450 °C over 2 h.

Figure 4 shows the *J–E* curves of the Ga_2O_3 thin films at various annealing temperatures and times. The leakage current was the largest and smallest when the films were annealed at 450 °C over 2 h and at 450 °C for 0.5 h, respectively. Thus, annealing time and leakage current density are positively associated with each other.

Figure 4 also shows the *I–V* curves of the Ga_2O_3 thin films at various annealing temperatures and times. The results indicate a diode effect for all parameters. The films had critical voltages of 2, 3, 17, and 3.5 V when annealed at 450 °C over 2 h, 450 °C over 1 h, 450 °C over 0.5 h, and 350 °C over 2 h, respectively. Finally, the reverse saturation current was the largest and smallest when the films were annealed at 450 °C over 0.5 h and 350 °C over 2 h, respectively. The Ga_2O_3 thin films may be used as a thin-film transistor or sensor.

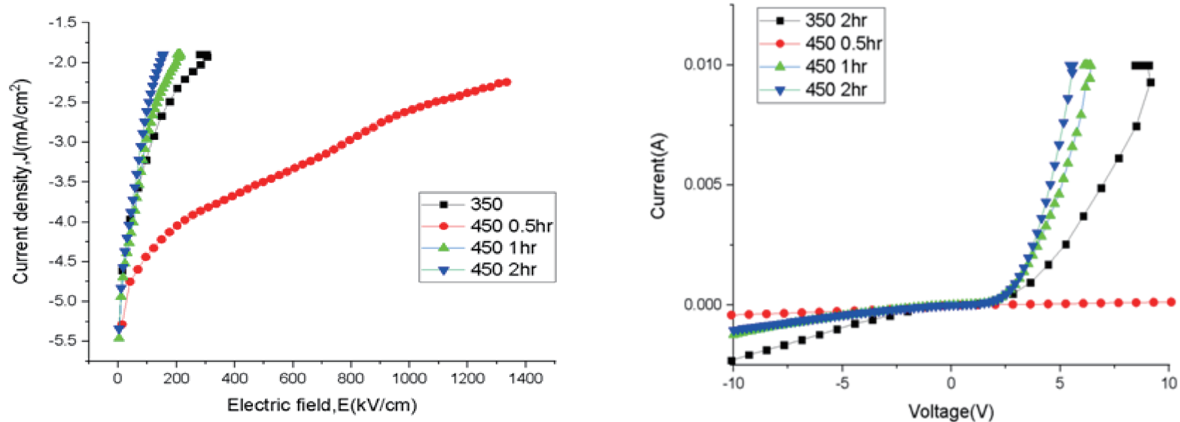

Fig. 4. (Color online) J–E and I–V curves of Ga_2O_3 films at various annealing temperatures and times.

4. Conclusions

Ga_2O_3 thin films were prepared by thermal evaporation, and their characteristics at different annealing temperatures and times were analyzed. XRD results indicated that the peak value was optimal when the films were annealed at 450 °C over 2 h. The peak at 35° was more pronounced at higher annealing temperatures, likely owing to the presence of the aluminum oxide phase in the films. According to results on the surface morphology and structure of the films, more fine particles are present at higher temperatures, and thicker films have more uneven surfaces. These particles and uneven surfaces considerably affect the electrical properties of the films. Gallium oxide thin films are suitable for use in active layers of oxygen sensors.

Acknowledgments

This work was supported by the National Science and Technology Council of the Republic of China under grants nos. NSTC 113-2221-E-239-010 and NSTC 112-2622-E-239-006.

References

1 C.-H. Huang, R.-H. Cyu, Y.-L. Chueh, and K. Nomura: Nat. Commun. **16** (2025) 1882. https://doi.org/10.1038/s41467-025-57200-2
2 D. Hu, S. Zhuang, Z. Ma, X. Dong, G. Du, B. Zhang, Y. Zhang, and J. Yin: J. Mater. Sci. Mater. Electron. **28** (2017) 10997. https://doi.org/10.1007/s10854-017-6882-x
3 Q. N. Abdullah, F. K. Yam, K. H. Mohmood, Z. Hassan, M. A. Qaeed, M. Bououdina , M. A. Almessiere, A. L. Al-Otaibi, and S. A. Abdulateef: Ceram. Int. **42** (2016) 13343. https://doi.org/10.1016/j.ceramint.2016.04.165
4 Q. Shi, Q. Wang, D. Zhang, Q. Wang, S. Li, W. Wang, Q. Fan, and J. Zhang: J. Luminescence **206** (2019) 53. https://doi.org/10.1016/j.jlumin.2018.10.005
5 R. Jangir, T. Ganguli, P. Tiwari, S. Porwal, H. Srivastava, S. K. Rai, B. Q. Khattak, and S. M. Oak: Appl. Surf. Sci. **257** (2011) 9323. https://doi.org/10.1016/j.apsusc.2011.05.039
6 M. Ogita, K. Higo, Y. Nakanishi, and Y. Hatanaka: Appl. Surf. Sci. **175** (2001) 721. https://doi.org/10.1016/S0169-4332(01)00080-0